NATIONAL ADVISORY COMMITTEE FOR AERONAUTICS

TECHNICAL NOTE 4168

A METHOD FOR CALCULATION OF HYDRODYNAMIC LIFT FOR SUBMERGED AND PLANING RECTANGULAR LIFTING SURFACES

By Kenneth L. Wadlin and Kenneth W. Christopher

Langley Aeronautical Laboratory
Langley Field, Va.

Washington
January 1958

U

NATIONAL ADVISORY COMMITTEE FOR AERONAUTICS

TECHNICAL NOTE 4168

A METHOD FOR CALCULATION OF HYDRODYNAMIC LIFT FOR SUBMERGED AND PLANING RECTANGULAR LIFTING SURFACES

By Kenneth L. Wadlin and Kenneth W. Christopher

SUMMARY

A method is presented for the calculation of lift coefficients for rectangular lifting surfaces of aspect ratios from 0.125 to 10 operating at finite depths beneath the water surface, including the zero depth or the planing condition. The theoretical expression for the lift coefficient is made up of a linear term derived from lifting-line theory and a nonlinear term from consideration of the effects of crossflow. The crossflow drag coefficient is assumed to vary linearly from a maximum at an aspect ratio of 0 to zero at an aspect ratio of 10. Theoretical values are compared with experimental values obtained at various depths of submersion with lifting surfaces having aspect ratios of 0.125, 0.25, 1.00, 4, 6, and 10.

The method of calculation is also applicable to hydrofoils having dihedral where the dihedral hydrofoil is replaced by a zero dihedral hydrofoil operating at a depth of submersion equal to the depth of submersion of the center-of-load location on the semispan of the dihedral hydrofoil.

Lift coefficients computed by this method are in good agreement with existing experimental data for aspect ratios from 0.125 to 10 and dihedral angles up to 30°.

INTRODUCTION

Hydro-skis and hydrofoils for water-based aircraft operate over a wide range of conditions from deep submergence to intersection with the water surface. With nonseparated flows and large depths, available aerodynamic theories apply directly to the hydrodynamic case, including those for fractional aspect ratios (ref. 1). For the zero depth or planing condition, a number of semiempirical methods exist for calculating the forces (ref. 2). At shallow depths, the effects of the water

surface must be taken into account, and rigorous methods for predicting the lift and drag of hydrofoils as they approach the water surface have been developed (ref. 3).

Considerations of the research outlined indicate that a theory is attainable for all practical aspect ratios and any depth including the planing condition. It also appears possible to include the effects of hydrofoil dihedral by considering the varying influence of depth over the span. This paper presents such a theory for the lift of a rectangular plan-form element and a correlation with experimental results obtained previously.

SYMBOLS

A	aspect ratio
a_o	two-dimensional lift-curve slope
b	span, ft
$C_{D,c}$	crossflow drag coefficient
C_L	total lift coefficient
$C_{L,c}$	nonlinear (crossflow) component of lift coefficient
$C_{L,l}$	linear component of lift coefficient
c	chord
d	depth of submersion of midthickness of leading edge for flat plate or leading edge on chord line for hydrofoils, chords
d'	depth of submersion of highest point on upper surface of lifting surface, in.
f	effective depth of quarter-chord, chords
f_t	depth of quarter-chord at tip, chords
K_2	two-dimensional depth correction factor
K_3	three-dimensional depth correction factor

l_m	mean wetted length, ft
α	angle of attack, radians unless otherwise stated
α_i	induced angle of attack, radians
$\alpha_{L=0}$	angle of attack at zero lift, deg
Γ	angle of dihedral, deg
Γ_c	circulation

THEORY

Linear Component of Lift

The general equation given by aerodynamic linear theory for the lift coefficient of an airfoil is

$$C_{L,l} = a_o(\alpha - \alpha_i) \tag{1}$$

where a_o is the two-dimensional lift-curve slope for a thin wing, α is the geometric angle of attack, and α_i is the induced angle of attack. Equation (1) is modified by Jones in reference 4 where the effect of aspect ratio on the edge velocity is considered. The equation for the lift coefficient presented by Jones is

$$C_{L,l} = \frac{a_o}{E}(\alpha - \alpha_i) \tag{2}$$

where E is the edge-velocity correction factor and is expressed as the ratio of the semiperimeter of the lifting surface to its span (for an elliptical plan form). Using this ratio for a rectangular lifting surface results in

$$E = \frac{A + 1}{A} \tag{3}$$

Using the value of α_i for elliptical loading $\left(\alpha_i = \frac{C_{L,l}}{\pi A}\right)$, equation (2) becomes

$$C_{L,l} = \frac{a_o \pi A \alpha}{\pi A + \pi + a_o} \tag{4}$$

and with $a_o = 2\pi$

$$C_{L,l} = \frac{2\pi A \alpha}{A + 3} \tag{5}$$

This, therefore, is the equation for the lift coefficient of a rectangular airfoil or deeply submerged hydrodynamic lifting surface given by the lifting-line theory as corrected by Jones (ref. 4). Equation (5) results in the same lift-curve slope for a rectangular wing of finite aspect ratio as given in reference 5.

Nonlinear Component of Lift

Lifting surfaces of low aspect ratio have a nonlinear lift-curve slope that is attributed to an additional component of lift due to the effects of crossflow (ref. 6). The crossflow component of the lift coefficient is expressed as

$$C_{L,c} = C_{D,c} \sin^2\alpha \cos \alpha \tag{6}$$

where $C_{D,c}$ is the crossflow drag coefficient. Experiment has shown that the crossflow drag coefficient varies considerably with plan form and edge conditions. As a result the theoretical determination of this coefficient is very difficult and the simple cases that have been solved have not correlated with experiment. For example Rayleigh's classical value for a flat plate in cavity flow which corresponds to planing is 0.88, whereas planing experiment yields a value of 4/3 (ref. 2) for this case. For the submerged case, where (considering only crossflow) a dead-water region is present on the upper side of the lifting surface, an increase in the crossflow drag coefficient by a factor of approximately 2 may be expected (ref. 7). In view of this, the value of 8/3, or twice the experimental planing value, is assumed for the submerged condition. For high aspect ratios, the linear theory alone predicts the value of lift coefficient obtained experimentally and the addition of the crossflow component of lift coefficient results in values too large. To account for this situation, the crossflow drag coefficient is assumed to vary linearly with aspect ratio from a maximum value at $A = 0$ to zero at $A = 10$. The crossflow component of lift is then expressed as

$$C_{L,c} = \frac{8}{3}\left(1 - \frac{A}{10}\right) \sin^2\alpha \cos \alpha \tag{7}$$

and the total lift coefficient for an airfoil or a deeply submerged hydrodynamic lifting surface is given by

$$C_L = \frac{2\pi A\alpha}{A + 3} + \frac{8}{3}\left(1 - \frac{A}{10}\right) \sin^2\alpha \cos \alpha \tag{8}$$

Effects of Depth of Submersion

Correction factors.- As the depth of submersion of a fully wetted hydrodynamic lifting surface is decreased, the lift coefficient decreases owing to the free-water surface boundary and approaches a minimum as the leading edge approaches the water surface. When the leading edge penetrates the water surface, the lifting surface enters the planing condition.

The equation for the lift coefficient can be corrected to include the effect of the free-water surface by applying two-dimensional and three-dimensional correction factors. The two-dimensional depth correction factor K_2 is determined by considering the effect at the three-quarter chord of a submerged two-dimensional lifting surface of an image line vortex located a distance above the water surface equal to the depth of submergence of the quarter-chord of the lifting surface. The vorticity of both the lifting surface and its image are located at their respective quarter-chords. The equation for K_2 for small angles of attack (where the quarter-chord and the three-quarter chord are essentially at the same depth) is given in reference 3 and is expressed as

$$K_2 = \frac{(4f)^2 + 1}{(4f)^2 + 2} \tag{9}$$

where f is the depth of the quarter-chord in chords. (The correction factor K_2 is expressed in ref. 3 as the ratio of the lift-curve slopes a_{o_2}/a_{o_1}, where the subscripts 1 and 2 refer to infinite and finite depths of submergence, respectively.) For small aspect ratios, the effect of angle of attack on the depth correction becomes appreciable since the difference in depth of the quarter-chord and the three-quarter chord becomes significant because of the relative increase in chord length and the higher angles of attack utilized. The following expression for K_2 which includes the effect of angle of attack was used for all lift-coefficient calculations:

$$K_2 = \frac{(4f)^2 + 8f \sin \alpha + 1}{(4f)^2 + 8f \sin \alpha + 2} \tag{10}$$

According to equation (10) with f defined as the depth of the quarter-chord, K_2 reaches its limiting value when the quarter-chord of the lifting surface reaches the free-water surface. Since the limiting value of K_2 corresponds to the border condition between planing and submerged flow, the value of f should become zero when the leading edge reaches the water surface. In order to satisfy this condition, the value of f is defined as

$$f = d + \frac{d \frac{c}{4} \sin \alpha}{0.05 + d} \tag{11}$$

where d is the depth of the midthickness of the leading edge in chords. The difference in the value of f as defined in equation (11) and the actual value of the depth of the quarter-chord is negligible for depths greater than 0.2 chord. As the depth of the quarter-chord is decreased below 0.2 chord, the defined values of f become increasingly smaller than the actual values of the quarter-chord depth and become zero at the quarter-chord depth of $\frac{c}{4} \sin \alpha$.

The three-dimensional correction factor K_3 is determined by considering the effect of an image horseshoe vortex on the lift of a submerged three-dimensional lifting surface. The equation for K_3 is presented in reference 3 (wherein K_3 is given in eq. (8) as the ratio Γ_2/Γ_1, where Γ_1 is the circulation at infinite depth and Γ_2 is the circulation at finite depth) as

$$K_3 = \frac{1}{1 + \frac{w_6}{w_5}} \tag{12}$$

where w_5 is the vertical component of the induced velocity at the three-quarter chord due to the horseshoe vortex of the hydrofoil and w_6 is the similar velocity component due to the image horseshoe vortex. The induced velocities w_5 and w_6 are defined in reference 3 neglecting angle of attack. Inclusion of the effect of angle of attack results in

$$w_5 = \frac{\Gamma_c}{\pi\sqrt{\frac{1}{4}+\frac{A^2}{4}}}\left\{\left(\frac{A}{2}\cos\alpha\right) + \frac{A}{4\left[\frac{A^2}{4}+\left(\frac{1}{2}\sin\alpha\right)^2\right]}\left(\frac{\cos\alpha}{2}+\sqrt{\frac{1}{4}+\frac{A^2}{4}}\right)\right\} \quad (13)$$

and

$$w_6 = \frac{\Gamma_c A}{4\pi\sqrt{\left(2f+\frac{1}{2}\sin\alpha\right)^2+\left(\frac{1}{2}\cos\alpha\right)^2+\frac{A^2}{4}}}\left(\left\{\frac{\cos\alpha}{2\left[\left(\frac{1}{2}\cos\alpha\right)^2+\left(2f+\frac{1}{2}\sin\alpha\right)^2\right]}\right\} + \left[\frac{1}{\frac{A^2}{4}+\left(2f+\frac{1}{2}\sin\alpha\right)^2}\right]\left[\frac{1}{2}\cos\alpha+\sqrt{\left(2f+\frac{1}{2}\sin\alpha\right)^2+\left(\frac{1}{2}\cos\alpha\right)^2+\frac{A^2}{4}}\right]\right) \quad (14)$$

The values for K_2 and K_3 for a few typical aspect ratios have been computed and are shown in figures 1 and 2. For a comparison between aspect ratios, the values for K_2 and K_3 at an angle of attack of 8° are shown in figure 3.

The two-dimensional lift-curve slope in equation (4) is multiplied by the two-dimensional depth correction factor K_2; this results in

$$C_{L,l} = \frac{2\pi K_2 A\alpha}{A + 2K_2 + 1} \quad (15)$$

The total lift coefficient corrected for depth of submersion is obtained by adding equations (7) and (15) and multiplying the sum by K_3; this results in

$$C_L = \frac{2K_2K_3\pi A\alpha}{A + 2K_2 + 1} + K_3\frac{8}{3}\left(1 - \frac{A}{10}\right)\sin^2\alpha\cos\alpha \quad (16)$$

Dihedral.- For a lifting surface of high aspect ratio having dihedral, the correction for depth of submergence varies along the span. Because of the spanwise distribution of loading, the correction for depth of submersion of the hydrofoil sections near the tip has less influence on the overall correction factor than does the correction at the root section where the load is more concentrated. In order to avoid the complication of using lifting-surface theory to account for this distribution of lift, an elliptical lift distribution is assumed and the dihedral hydrofoil is replaced by a zero-dihedral hydrofoil operating at a depth of submersion equal to the depth of submersion of the center-of-load location on the semispan of the dihedral hydrofoil. The depth of submersion of the equivalent flat hydrofoil is then

$$f = f_t + \frac{A}{2} \tan \Gamma \left(1 - \frac{4}{3\pi}\right) \tag{17}$$

where f_t is the depth of submersion of the quarter-chord at the tip of the hydrofoil. Values of K_2 and K_3 are then obtained from equations (10) and (12) by using values of f from equation (17).

Since the crossflow term is dependent on conditions at the tip of the hydrofoil, the correction factor for the crossflow term is obtained by using the depth of submersion of the tip of the hydrofoil. The total lift coefficient of the dihedral hydrofoil is then written as

$$C_L = \frac{2K_2K_3\pi A\alpha}{A + 2K_2 + 1} + K_{3,t} \frac{8}{3} \left(1 - \frac{A}{10}\right) \sin^2\alpha \cos \alpha \tag{18}$$

where $K_{3,t}$ is obtained from equation (12) by using the depth of submersion of the tip of the hydrofoil.

Planing.- As seen in figures 1 and 2, the limiting value of K_2 and K_3 for zero depth of submergence is 0.5. Therefore, the theoretical lift coefficient corrected for the effect of depth of submergence (eq. (16)) becomes, at zero depth of submergence,

$$C_L = \frac{0.5\pi A\alpha}{A + 2} + \frac{4}{3} \left(1 - \frac{A}{10}\right) \sin^2\alpha \cos \alpha \tag{19}$$

However, at zero depth of submergence, the lifting surface starts to plane and certain changes in the flow condition must be considered. Since there is no flow over the top of the lifting surface in the planing condition and therefore no circulation, the induced angle of attack is dropped from equation (1) so that, for the planing condition,

$$C_{L,l} = \frac{0.5\pi A\alpha}{A + 1} \tag{20}$$

Because of the absence of flow over the top of the lifting surface, no leading-edge suction acts on the lifting surface. In the strictest sense the suction component of lift should be based only on the linear term; however, comparison of experiment with theory (ref. 2) indicates that better agreement is obtained if the suction component is based on both terms of the lift equation. Therefore, the leading-edge suction $\left(C_L \sin^2\alpha\right)$ is removed from both terms of the lift coefficient so that the final equation for the lift coefficient of a rectangular plan-form lifting surface in the planing condition is

$$C_L = \frac{0.5\pi A\alpha}{A + 1} \cos^2\alpha + \frac{4}{3}\left(1 - \frac{A}{10}\right) \sin^2\alpha \cos^3\alpha \tag{21}$$

where A is now the aspect ratio of the wetted portion of the lifting surface. Equation (21) is similar to the equation for the planing lift coefficient presented in reference 2 for a flat plate with sharp chines. The only difference in the two equations is the presence of the $\left(1 - \frac{A}{10}\right)$ term in the crossflow drag portion of the present equation. The difference in calculated values given by the two equations is less than 2.6 percent for length-beam ratios greater than 2 (aspect ratios less than 0.5) and angles of attack of 30° or less. The differences in values calculated by the two equations become smaller with decreasing angle of attack or increasing length-beam ratio.

Summary of Final Equations

The lift coefficient of submerged zero-dihedral surfaces is calculated from the following equation (which is eq. (16)):

$$C_L = \frac{2K_2K_3\pi A\alpha}{A + 2K_2 + 1} + K_3 \frac{8}{3}\left(1 - \frac{A}{10}\right) \sin^2\alpha \cos\alpha$$

where K_2 and K_3 are calculated from equations (10) and (12). For submerged surfaces having dihedral, equation (18)

$$C_L = \frac{2K_2K_3\pi A\alpha}{A + 2K_2 + 1} + K_{3,t}\frac{8}{3}\left(1 - \frac{A}{10}\right)\sin^2\alpha\cos\alpha$$

is used where K_2 and K_3 are calculated from equations (10) and (12) by using the depth of submersion calculated from equation (17) and where $K_{3,t}$ is calculated from equation (12) by using the depth of the tip of the lifting surface.

The lift coefficient of the basic flat-bottom planing surface with sharp chines is calculated from the following equation (which is eq.(21)):

$$C_L = \frac{0.5\pi A\alpha}{A + 1}\cos^2\alpha + \frac{4}{3}\left(1 - \frac{A}{10}\right)\sin^2\alpha\cos^3\alpha$$

If the chines are not sharp the coefficient of the second term (4/3) is reduced as pointed out in reference 2. In addition this reference provides a means for estimating the value of this coefficient for a variety of chine conditions and for taking into account the effects of dead rise.

COMPARISON OF THEORY AND EXPERIMENT

Submerged Surfaces

Zero-dihedral surfaces.- Experimental data from a series of modified flat plates with elliptical leading edges, beveled trailing edges, and square-cut side edges were used for comparison with theory for the low-aspect-ratio cases (A = 0.125, 0.25, and 1.00 (refs. 1 and 8)). The plates were mounted on an NACA 66_1-012 section strut attached near the center of the upper surface of the plate. The lifting surfaces were tested at constant depths of submersion measured from the free-water surface to the highest point on the lifting surface. As a result the depth of the quarter-chord varied with angle of attack. This variation of depth of the quarter-chord was taken into account in determining the values of the depth correction factors. Data for speeds of 25 and 30 feet per second were used to provide a useful range of data and thus the low speed range where some variation of lift coefficient with speed is indicated (ref. 1) was avoided. Comparisons between theoretical and experimental values of lift coefficient are presented in

figures 4 to 6. Good agreement between theory and experiment is indicated over most of the range of experimental data available.

A comparison between theoretical and experimental values of lift coefficient for a hydrofoil of aspect ratio 4 is shown in figure 7. The theoretical curves of lift coefficient are based on angles of zero lift calculated by the method given in reference 9. The hydrofoil used in the experimental investigation had an NACA 64_1A412 section profile as shown by the sketch in the figure. A sting mount was used to support the hydrofoil during the tests (ref. 3) so that the hydrofoil was positioned 1 foot forward of the supporting strut. The hydrofoil was tested at constant depths of submersion measured to the highest point of the upper surface of the hydrofoil. However, the variation in depth of the quarter-chord was less than 0.01 chord in the range of angles of attack used and was neglected. As can be seen, the theory is in good agreement with experiment.

A comparison between theoretical and experimental values of lift coefficient for a hydrofoil of aspect ratio 6 is presented in figure 8. Two sets of experimental data are presented for comparison. For the tests reported in reference 10 the hydrofoil (NACA 16,S-209 section) was mounted on 3 struts attached to the upper surface of the hydrofoil at the 1/4-, 1/2-, and 3/4-span positions. In the tests reported in reference 11 the center strut was eliminated. An NACA 16-509 section hydrofoil was used in the latter tests. In both sets of tests, depths of submergence were measured to the quarter-chord of the hydrofoil. Good agreement between theory and experiment is indicated.

Two sets of data have been obtained with an NACA 64_1A412 section hydrofoil of aspect ratio 10 and are reported in references 3 and 12. The tests were made in the Langley tank no. 2 and the experimental values of lift coefficient have been corrected in this paper to remove the effect of the proximity of the sides and bottom of the tank. The hydrofoil was mounted on a single strut attached at midspan to the upper surface of the hydrofoil. The depths of submergence were measured to the top surface of the hydrofoil; however, as in the case for the hydrofoil of aspect ratio 4, the variation in depth of the quarter-chord with change in angle of attack was negligible. A comparison between theoretical and experimental values of lift coefficient for a hydrofoil of aspect ratio 10 is shown in figure 9. As can be seen, good agreement between theory and experiment is indicated.

The variation of theoretical and experimental values of lift coefficient with depth at a constant angle of attack is shown in figures 10 and 11. The data points represent faired values for the angle of attack selected. For the cambered sections (fig. 11), the angle of attack was measured from the theoretical angle of zero lift.

The good agreement between calculated and experimental values seems to indicate that this method offers a means of calculating within engineering accuracy the lift coefficients of rectangular lifting surfaces of a wide range of aspect ratios operating at any depth of submersion.

Dihedral surfaces.- The dihedral-hydrofoil data were obtained from tests of a series of three hydrofoils of aspect ratio 6 (ref. 11). The dihedral hydrofoils were supported by 2 struts attached to the upper surface of the hydrofoil at the $\frac{1}{4}$- and $\frac{3}{4}$- span positions. The experimental angles of attack were measured about a horizontal axis perpendicular to the plane of symmetry of the hydrofoil. Since the true angle of attack of the hydrofoil is measured in a plane perpendicular to the chord plane, the true and experimental values agree only at $\alpha = 0^\circ$. Changes in true angle of attack from $\alpha = 0^\circ$ are smaller by the cosine of the dihedral angle than those measured during the experiment. Therefore, for comparison with experiment, the theoretical angles of attack were divided by the cosine of the dihedral angle. This results in a more negative angle for zero lift with increasing dihedral angle. Experimental and theoretical lift coefficients for the three hydrofoils operating at various fully submerged depths are shown in figures 12 to 14.

For dihedral angles of 30° or less, the method of calculation seems to predict with reasonable accuracy the lift of hydrofoils having dihedral and operating at any tip depth.

Planing Surfaces

Figure 15 shows a comparison between theoretical and experimental values of lift coefficient for a rectangular flat-bottom lifting surface in the planing condition. The experimental data were taken from references 2 and 13. The agreement between theory and experiment is, in general, good and indicates that the method of calculation can be used for calculating planing lift coefficients with reasonable accuracy.

A composite plot of theoretical and experimental lift coefficients throughout the planing and submerged range of depths for a flat plate of aspect ratio 0.25 at a constant angle of attack is shown in figure 16. As can be seen the lift coefficient decreases with decrease in depth of submersion and approaches a minimum as the leading edge approaches the water surface. A sudden increase in lift coefficient is indicated as the leading edge penetrates the water surface and is followed by a more gradual increase in lift coefficient with rise due to the resulting change in aspect ratio of the wetted area with rise.

The sudden increase in the computed values at the water surface is due to the fact that in the computations an instantaneous change

from the fully wetted condition to the separated flow condition was assumed to occur at this point. The two totally different flow regimes result in slightly different values for the lift coefficients. Experiment has shown (ref. 1) that as the leading edge of the lifting surface approaches very near the water surface the flow over the top separates at the leading edge and forms a bubble or blister over the top of the lifting surface. During this condition the lift coefficient is less than that predicted by the theory for either the planing or the submerged condition. Therefore the proposed method of calculating the lift coefficients can be expected to give only approximate values for a short range of shallow depths of submersion where separation occurs during the transition from the submerged to the planing condition.

SUMMARY OF RESULTS

The results of the theoretical investigation to determine a general method for calculation of lift for lifting surfaces may be summarized as follows:

1. A general method is presented for the calculation of lift coefficients of rectangular lifting surfaces of a wide range of aspect ratios operating at any depth of submersion beneath the surface of water.

2. The method of calculation is applicable to zero depth of submersion (planing condition) when the changes in flow conditions are taken into consideration.

3. The method can be used for the calculation of lift for hydrofoils having dihedral.

4. Lift coefficients computed by this method are in good agreement with existing experimental data for aspect ratios from 0.125 to 10 and dihedral angles up to 30°.

Langley Aeronautical Laboratory,
National Advisory Committee for Aeronautics,
Langley Field, Va., August 23, 1957.

REFERENCES

1. Wadlin, Kenneth L., Ramsen, John A., and Vaughan, Victor L., Jr.: The Hydrodynamic Characteristics of Modified Rectangular Flat Plates Having Aspect Ratios of 1.00, 0.25, and 0.125 and Operating Near a Free Water Surface. NACA Rep. 1246, 1955. (Supersedes NACA TN's 3079 by Wadlin, Ramsen, and Vaughan and 3249 by Ramsen and Vaughan.)

2. Shuford, Charles L., Jr.: A Theoretical and Experimental Study of Planing Surfaces Including Effects of Cross Section and Plan Form. NACA TN 3939, 1957.

3. Wadlin, Kenneth L., Shuford, Charles L., Jr., and McGehee, John R.: A Theoretical and Experimental Investigation of the Lift and Drag Characteristics of Hydrofoils at Subcritical and Supercritical Speeds. NACA Rep. 1232, 1955. (Supersedes NACA RM's L52D23a by Wadlin, Shuford, and McGehee and L51B13 by Wadlin, Fontana, and Shuford.)

4. Jones, Robert T.: Correction of the Lifting-Line Theory for the Effect of the Chord. NACA TN 817, 1941.

5. Wood, Karl D.: Technical Aerodynamics. Second ed., McGraw-Hill Book Co., Inc., 1947, p. 144.

6. Betz, A.: Applied Airfoil Theory. Airfoils or Wings of Finite Span. Vol. IV or Aerodynamic Theory, div. J, ch. III, sec. 7, W. F. Durand, ed., Julius Springer (Berlin), 1935 (reprinted by Durand Reprinting Committee, 1943), pp. 69-72.

7. Glauert, H.: The Elements of Aerofoil and Airscrew Theory. Second ed., Cambridge Univ. Press, 1947, p. 95. (Reprinted 1948.)

8. Vaughan, Victor L., Jr., and Ramsen, John A.: Hydrodynamic Characteristics Over a Range of Speeds Up to 80 Feet Per Second of a Rectangular Modified Flat Plate Having an Aspect Ratio of 0.25 and Operating at Several Depths of Submersion. NACA TN 3908, 1957.

9. Abbott, Ira H., Von Doenhoff, Albert E., and Stivers, Louis S., Jr.: Summary of Airfoil Data. NACA Rep. 824, 1945. (Supersedes NACA WR L-560.)

10. Land, Norman S.: Characteristics of an NACA 66,S-209 Section Hydrofoil at Several Depths. NACA WR L-757, 1943. (Formerly CB 3E27.)

11. Benson, James M., and Land, Norman S.: An Investigation of Hydrofoils in the NACA Tank. I - Effect of Dihedral and Depth of Submersion. NACA WR L-758, 1942. (Formerly NACA ACR, Sept. 1942.)

12. Wadlin, Kenneth L., Ramsen, John A., and McGehee, John R.: Tank Tests at Subcavitation Speeds of an Aspect-Ratio-10 Hydrofoil With a Single Strut. NACA RM L9K14a, 1950.

13. Weinstein, Irving, and Kapryan, Walter J.: The High-Speed Planing Characteristics of a Rectangular Flat Plate Over a Wide Range of Trim and Wetted Length. NACA TN 2981, 1953.

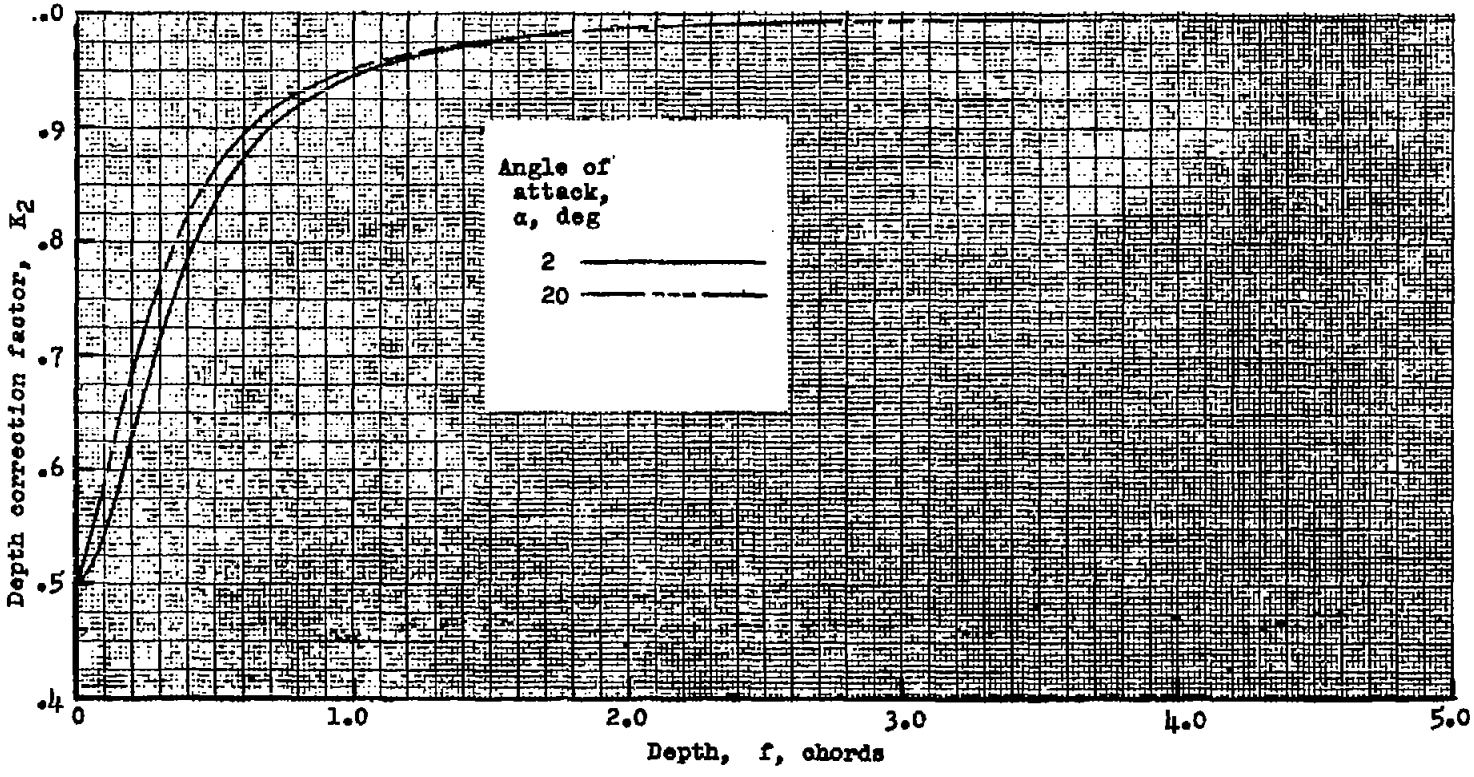

Figure 1.- Variation of the two-dimensional depth correction factor with depth.

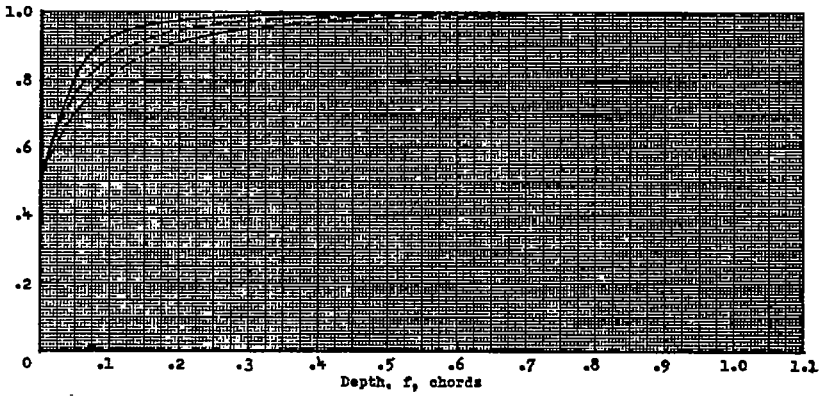

(a) A = 0.125.

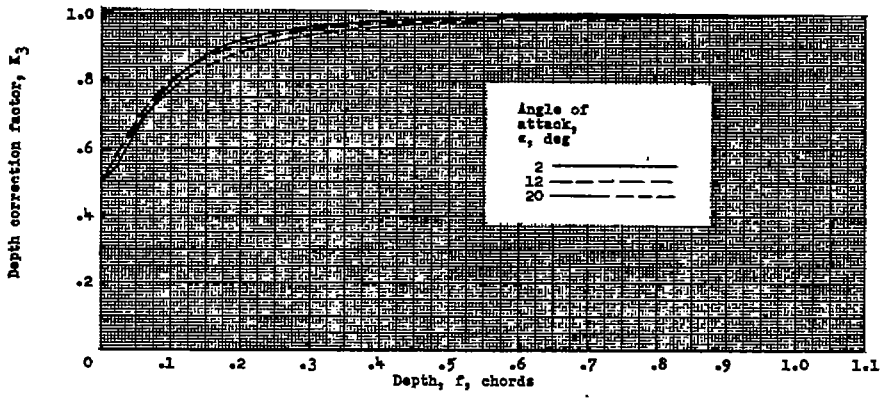

(b) A = 0.25.

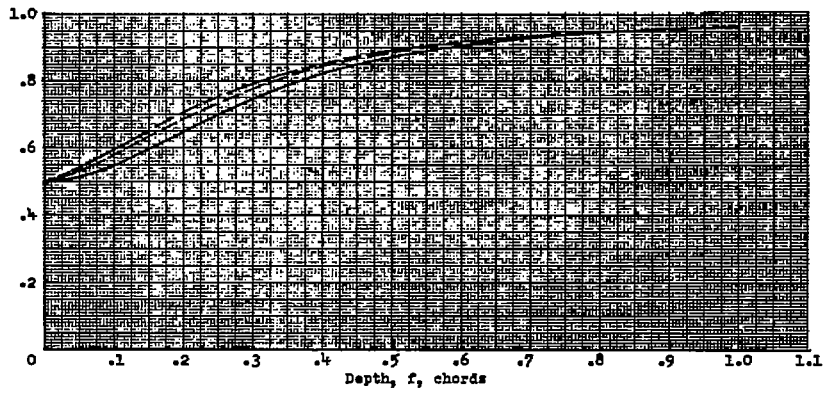

(c) A = 1.00.

Figure 2.- Variation of three-dimensional depth correction factor with depth.

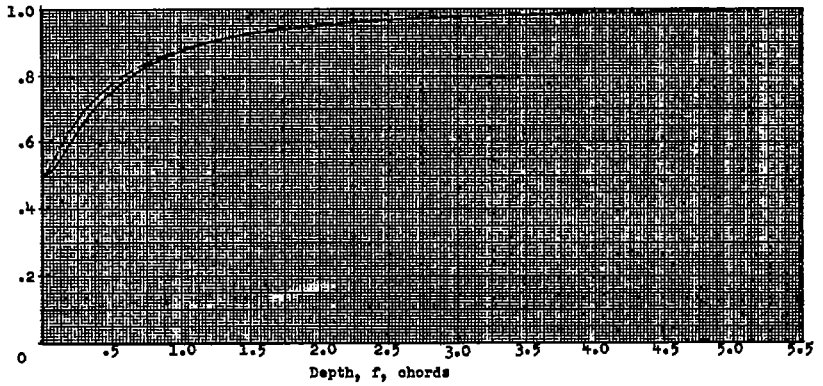

(d) A = 4.

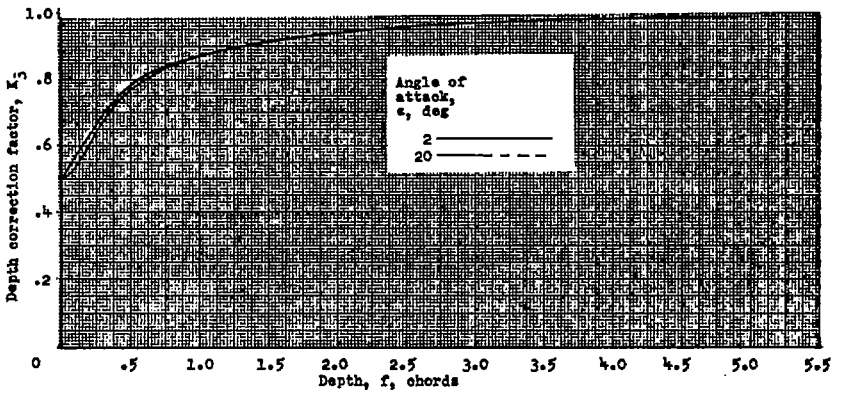

(e) A = 6.

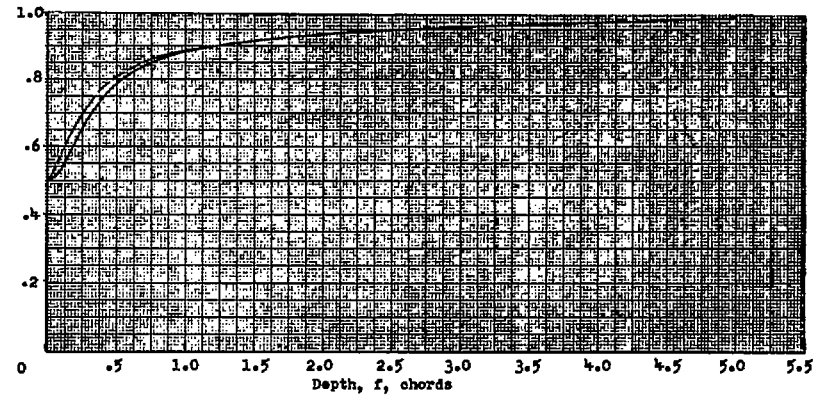

(f) A = 10.

Figure 2.- Concluded.

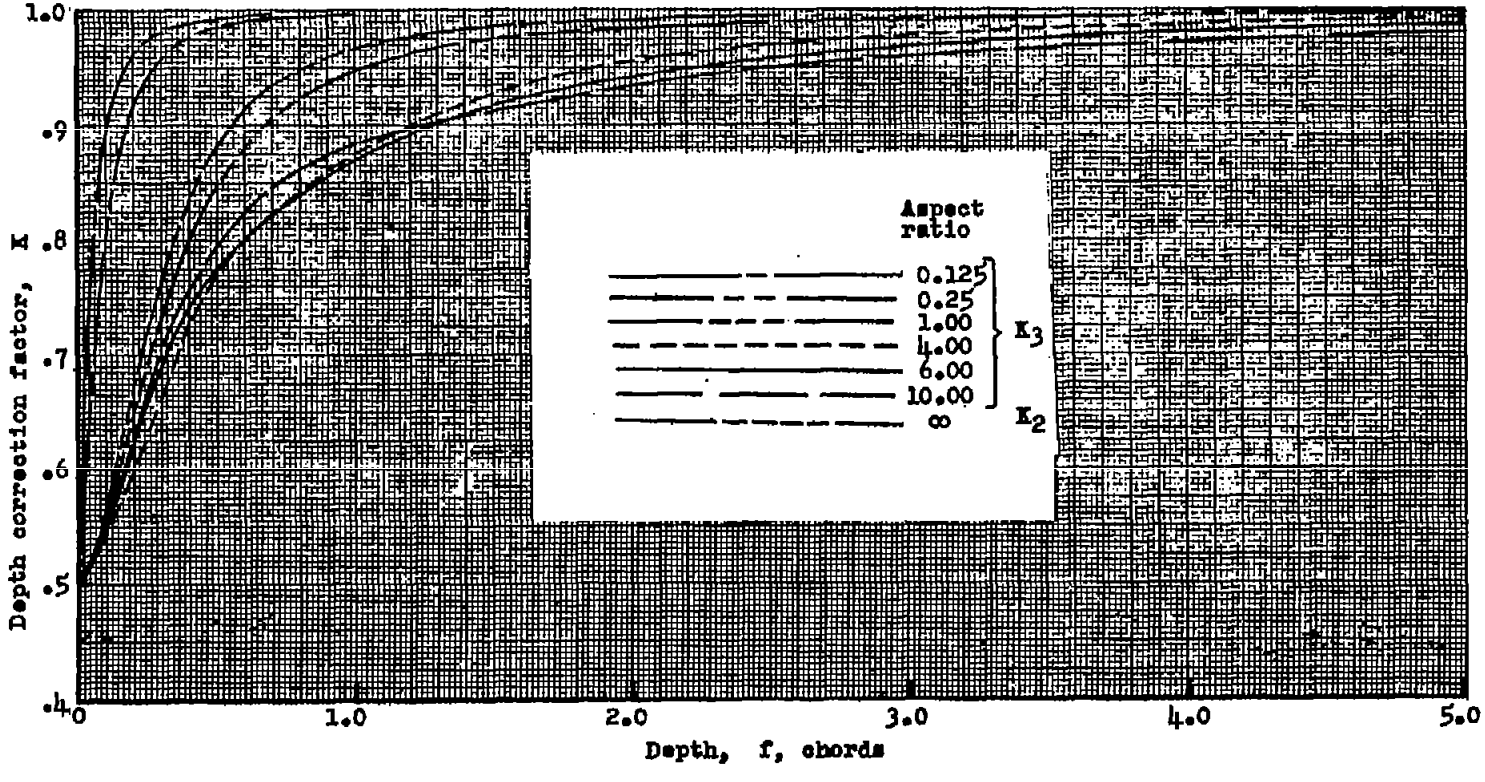

Figure 3.- Variation of depth correction factors with depth for typical aspect ratios at constant angle of attack. $\alpha = 8^{\circ}$.

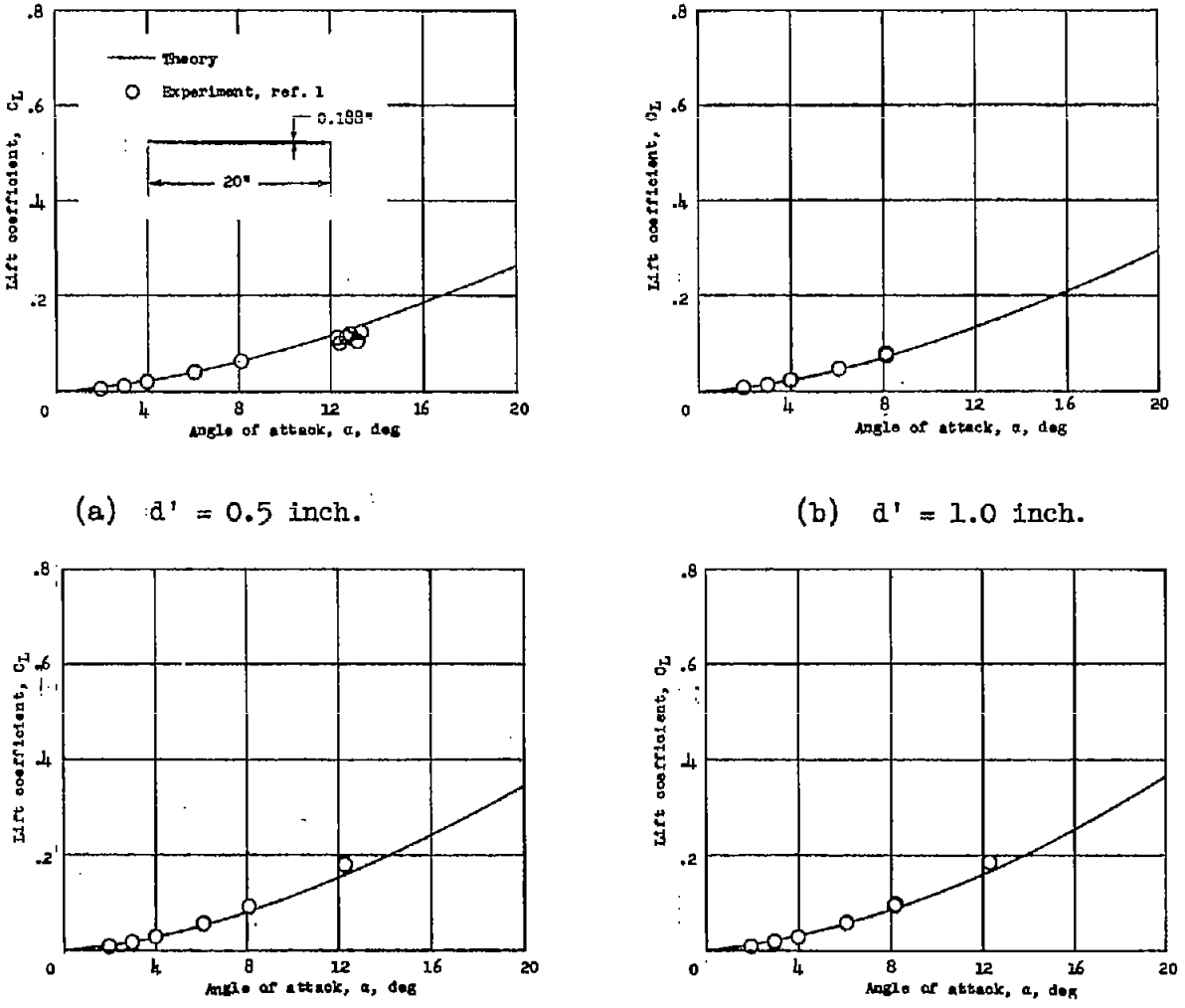

(a) d' = 0.5 inch.

(b) d' = 1.0 inch.

(c) d' = 3.0 inches.

(d) d' = 6.0 inches.

Figure 4.- Comparison of experimental and theoretical lift coefficients at various depths for a modified flat plate of aspect ratio 0.125.

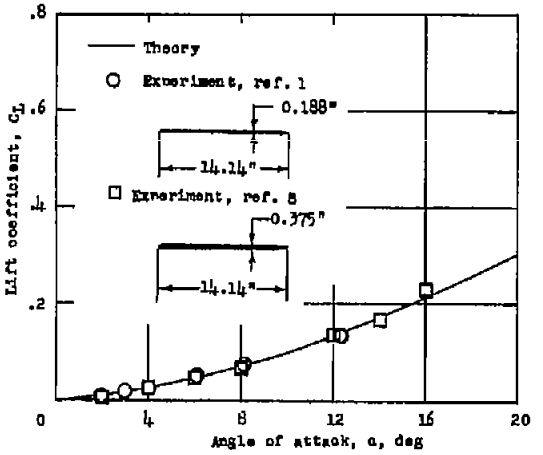

(a) d' = 0.5 inch.

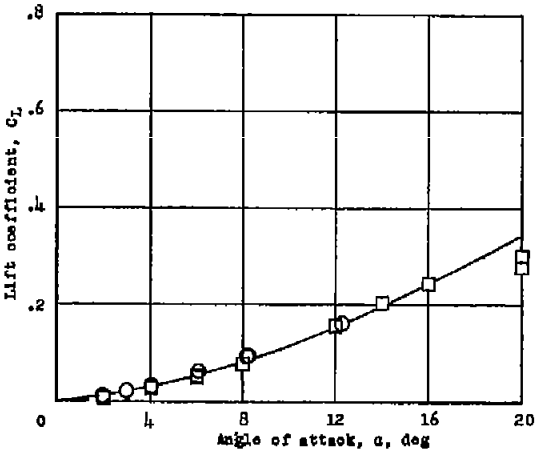

(b) d' = 1.0 inch.

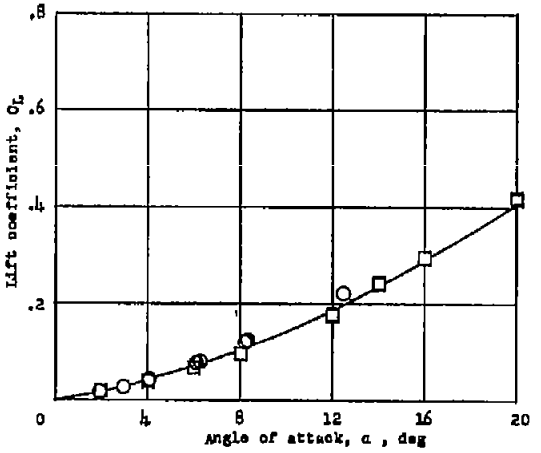

(c) d' = 3.0 inches.

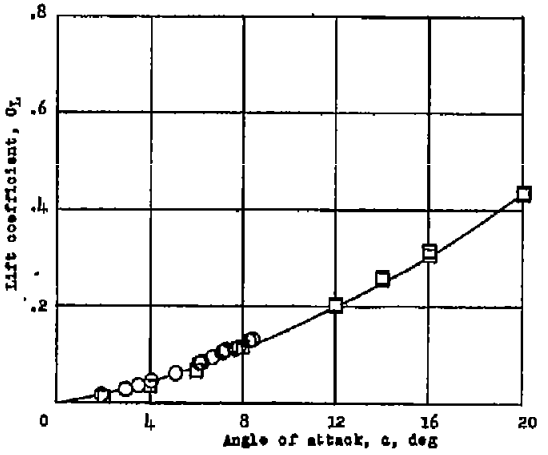

(d) d' = 6.0 inches.

Figure 5.- Comparison of experimental and theoretical lift coefficients at various depths for a modified flat plate of aspect ratio 0.25.

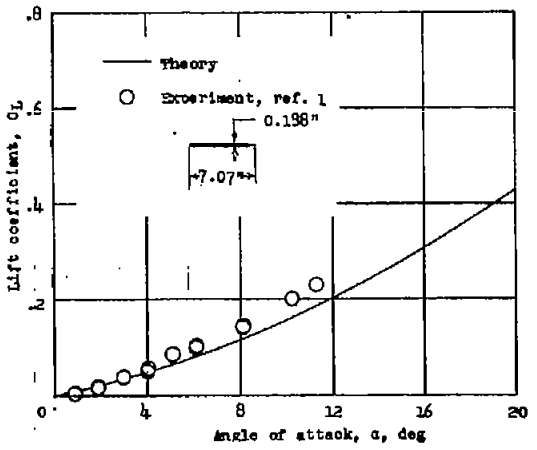

(a) d' = 0.5 inch.

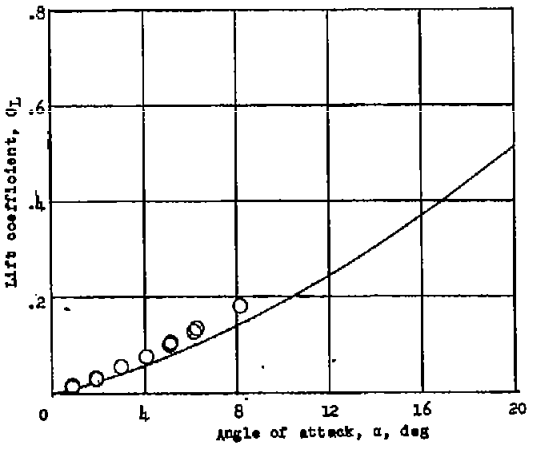

(b) d' = 1.0 inch.

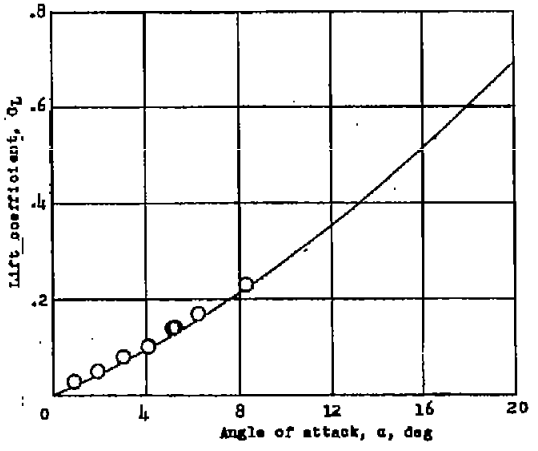

(c) d' = 3.0 inches.

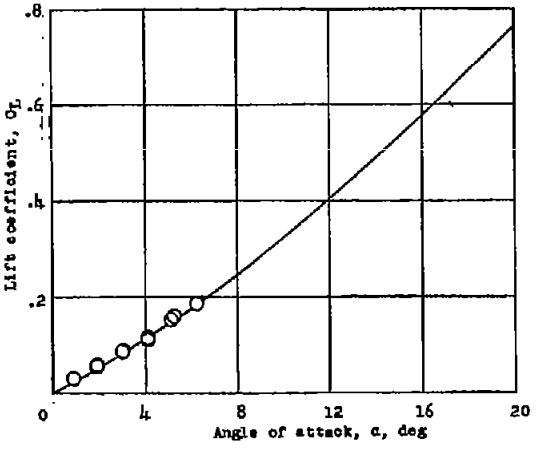

(d) d' = 6.0 inches.

Figure 6.- Comparison of experimental and theoretical lift coefficients at various depths for a modified flat plate of aspect ratio 1.00.

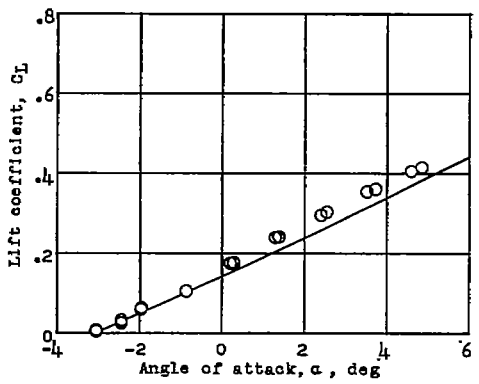

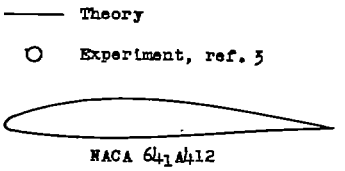

(a) f = 0.58 chord.

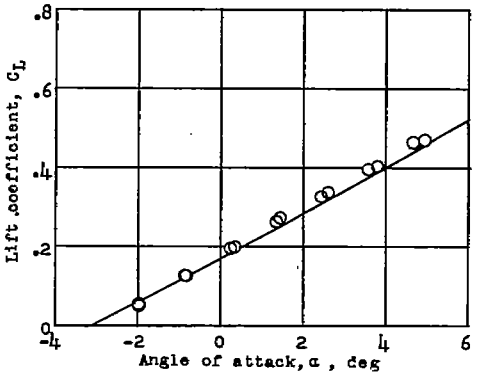

(b) f = 1.08 chords.

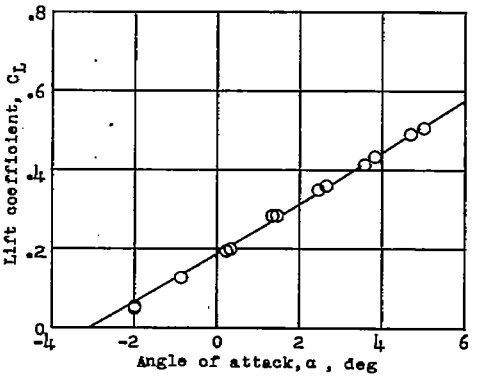

(c) f = 2.08 chords.

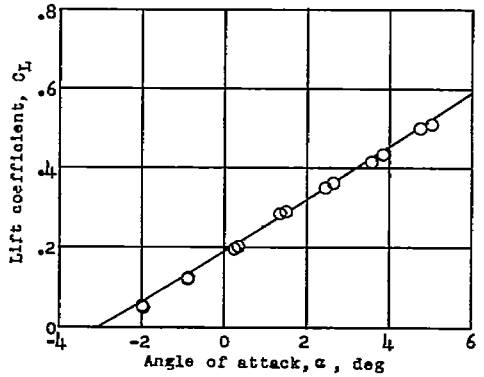

(d) f = 3.08 chords.

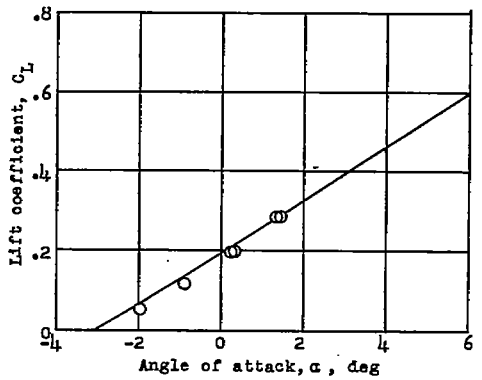

(e) f = 4.08 chords.

Figure 7.- Comparison of experimental and theoretical lift coefficients at various depths for a hydrofoil of aspect ratio 4.

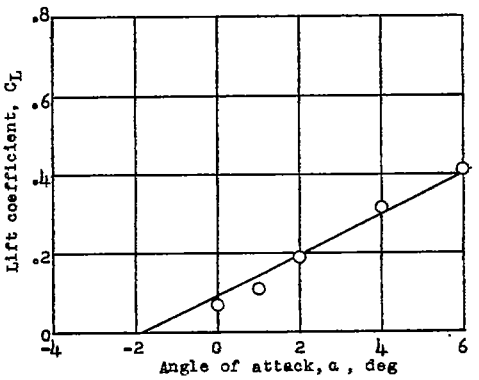

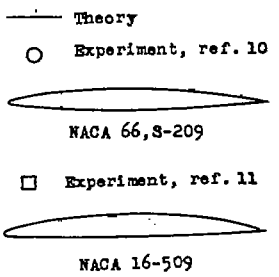

(a) f = 0.5 chord.

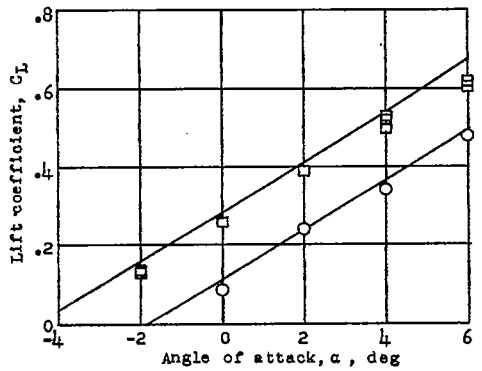

(b) f = 1.0 chord.

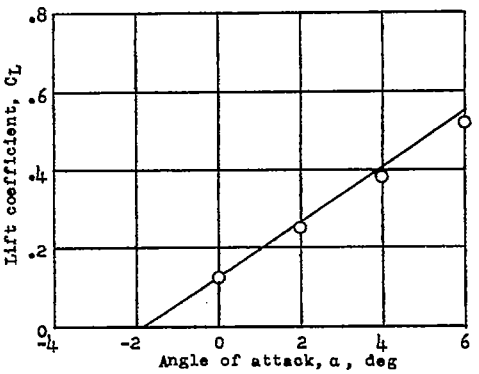

(c) f = 2.0 chords.

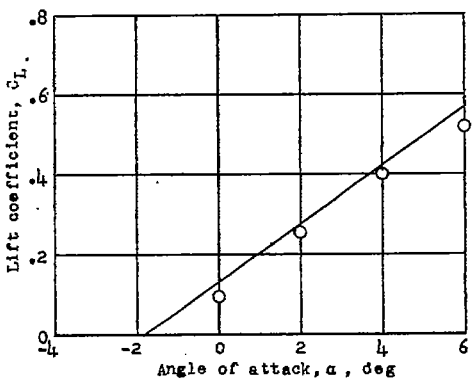

(d) f = 3.0 chords.

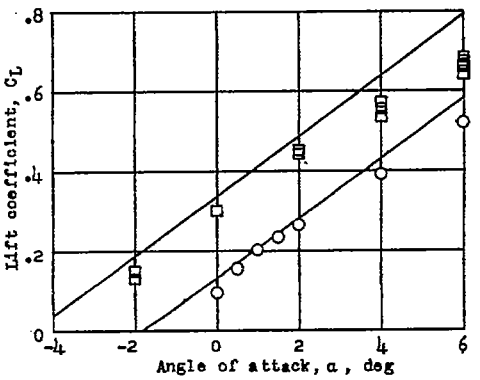

(e) f = 5.0 chords.

Figure 8.- Comparison of experimental and theoretical lift coefficients at various depths for a hydrofoil of aspect ratio 6.

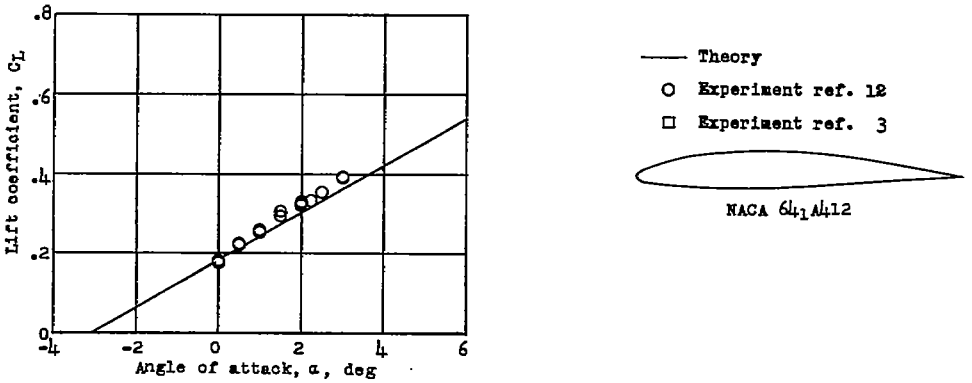

(a) f = 0.52 chord.

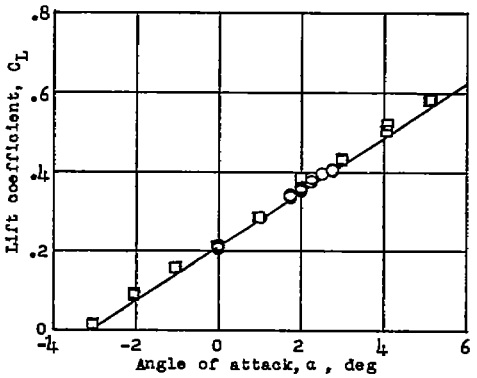

(b) f = 0.83 chord.

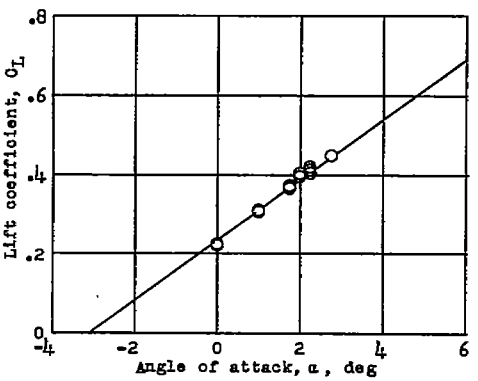

(c) f = 1.58 chords.

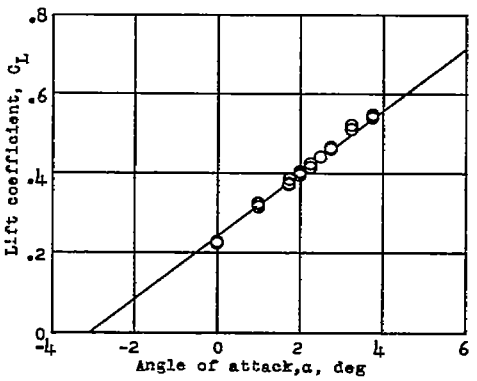

(d) f = 2.33 chords.

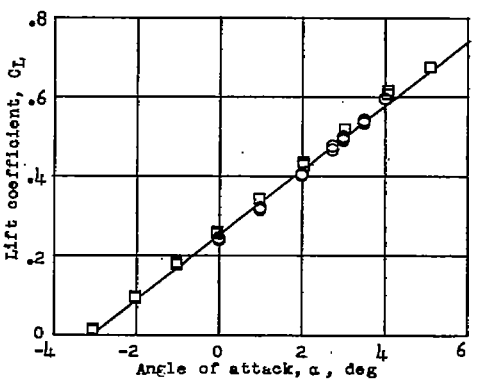

(e) f = 3.83 chords.

Figure 9.- Comparison of experimental and theoretical lift coefficients at various depths for a hydrofoil of aspect ratio 10.

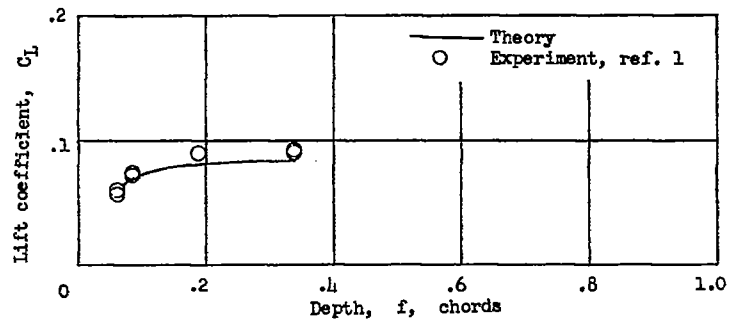

(a) A = 0.125.

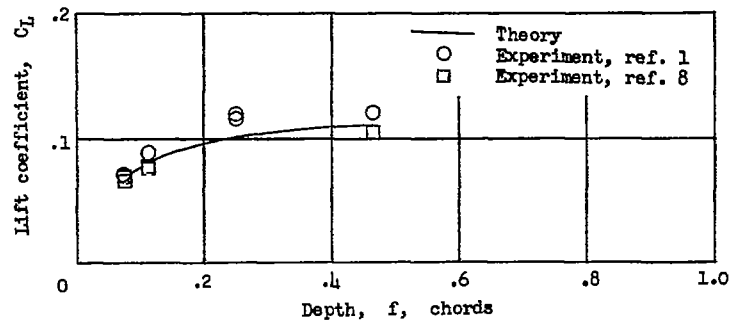

(b) A = 0.25.

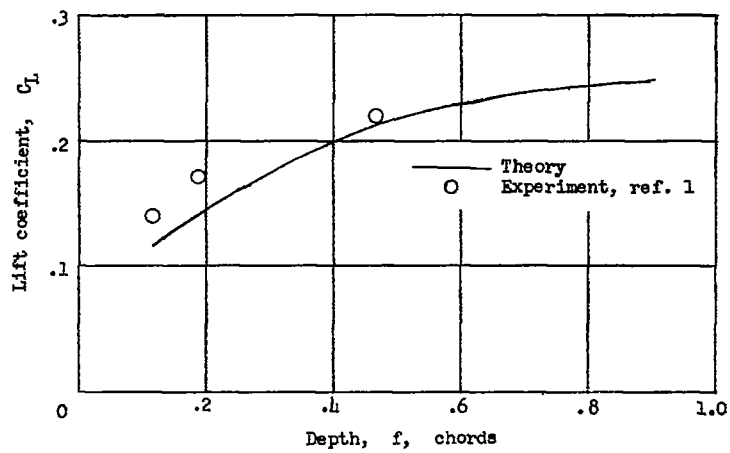

(c) A = 1.00.

Figure 10.- Variation of lift coefficient with depth for modified rectangular flat plates of different aspect ratios at constant angle of attack. $\alpha = 8^{\circ}$.

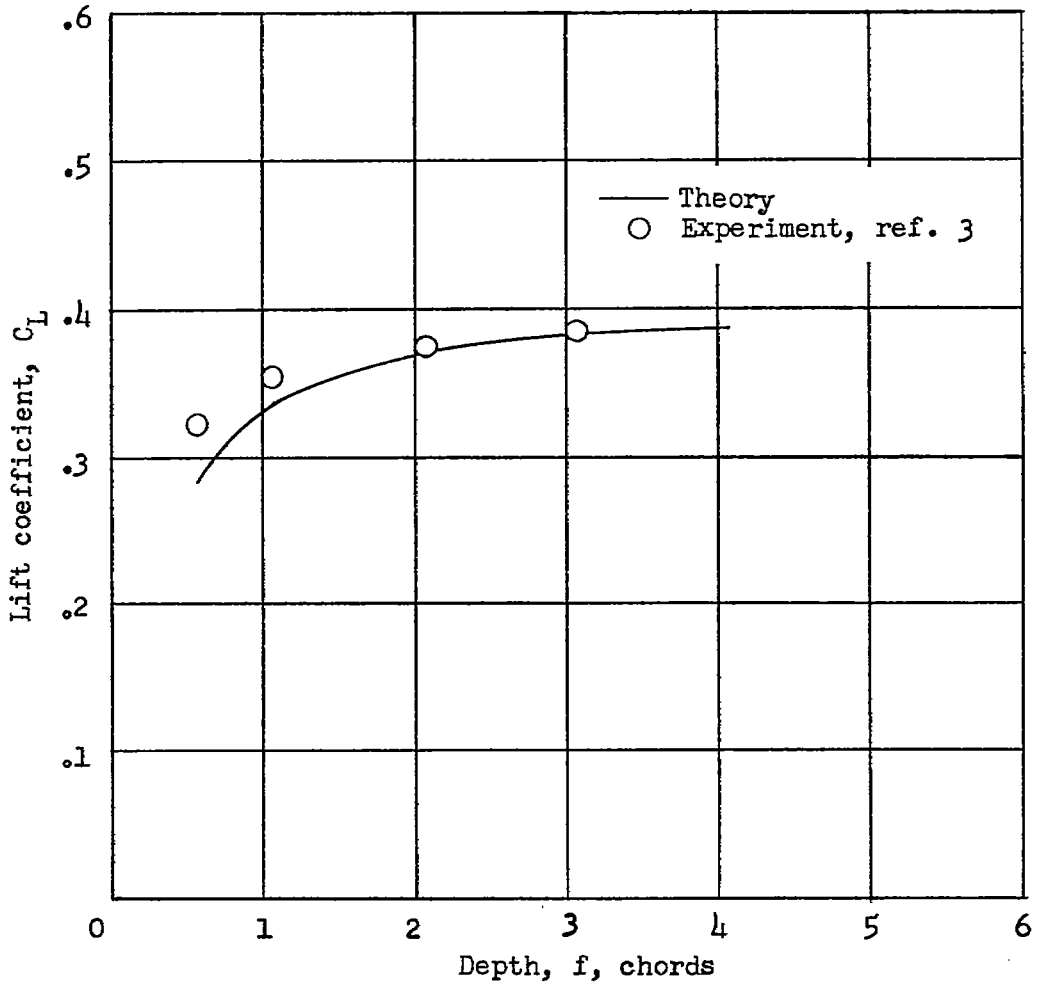

(a) A = 4.

Figure 11.- Variation of lift coefficient with depth for hydrofoils of different aspect ratios at constant angle of attack. $\alpha = \alpha_{L=0} + 6^{\circ}$.

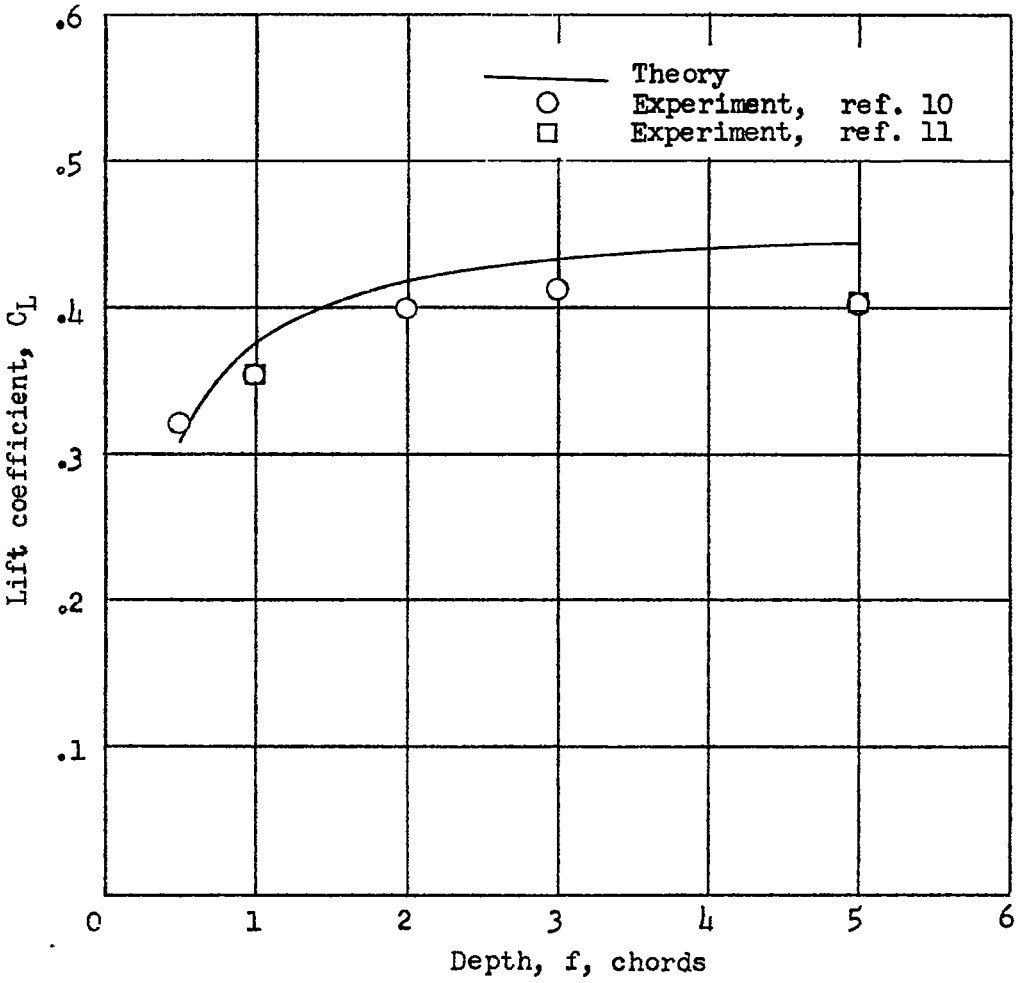

(b) A = 6.

Figure 11.- Continued.

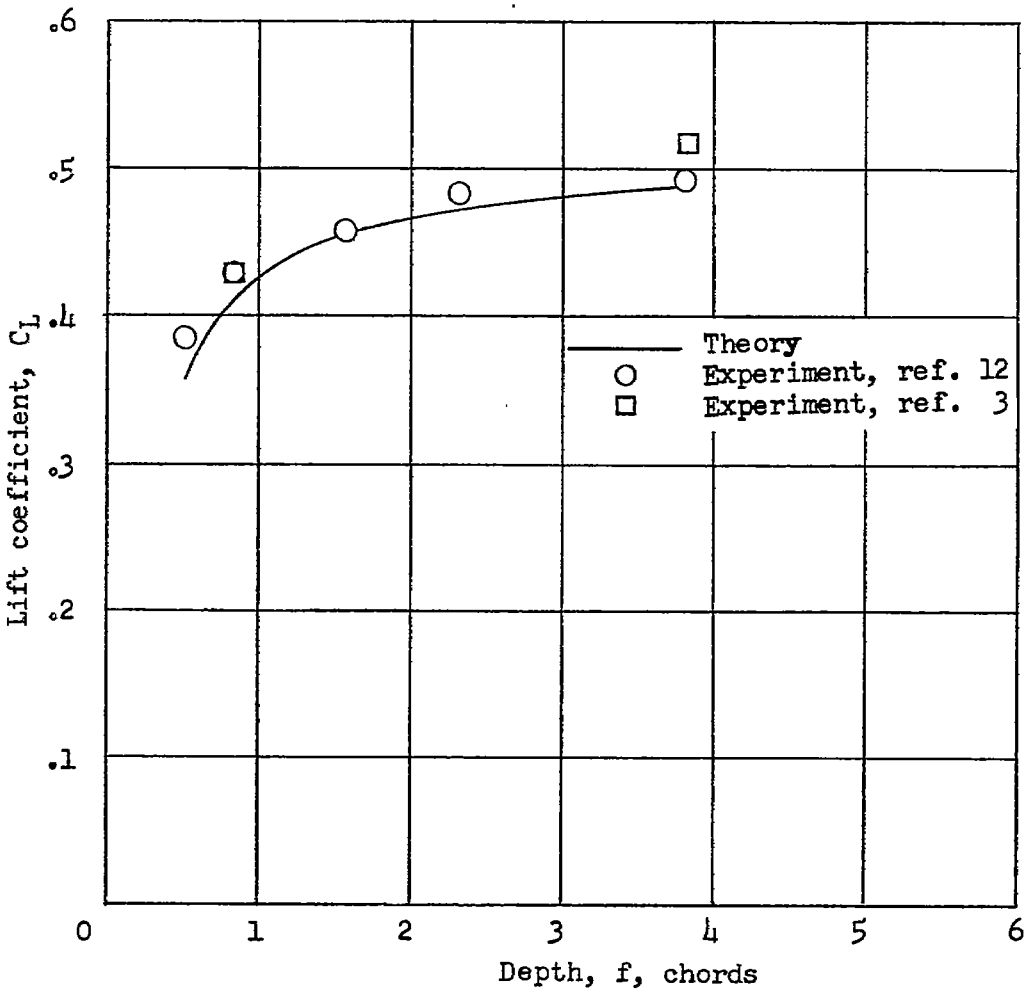

(c) A = 10.

Figure 11.- Concluded.

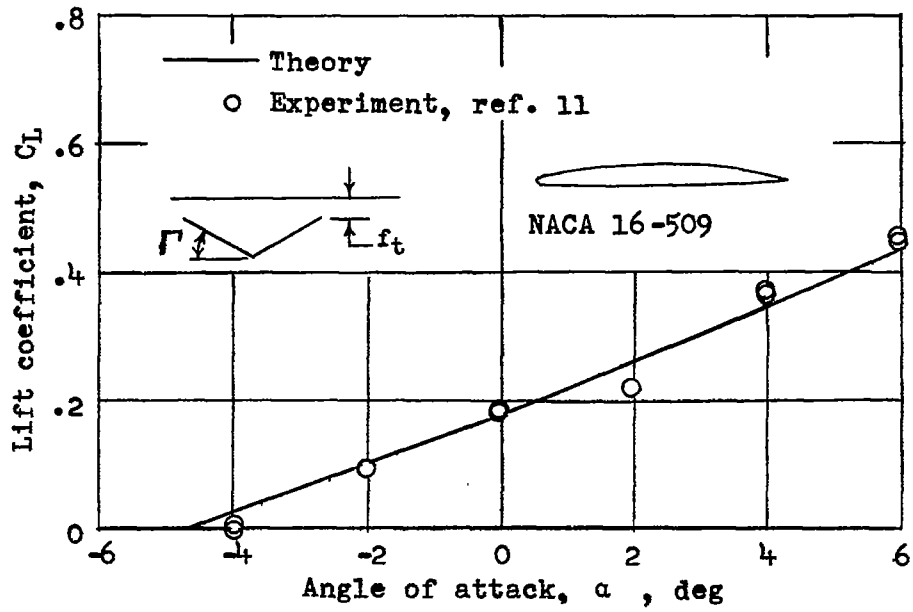

(a) f_t = 0 chord.

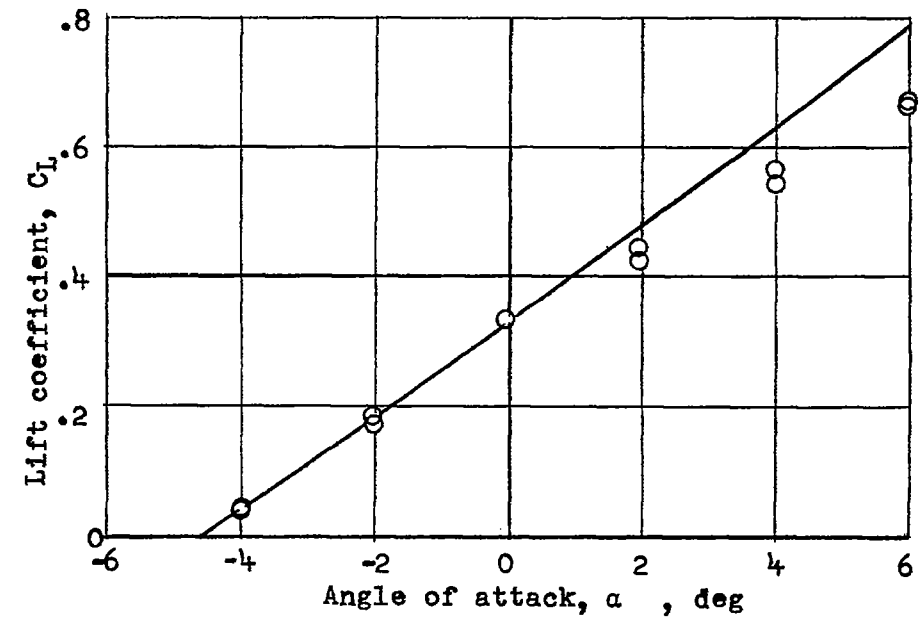

(b) f_t = 4.48 chords.

Figure 12.- Comparison of experimental and theoretical lift coefficients for a hydrofoil of aspect ratio 6 with 10° dihedral.

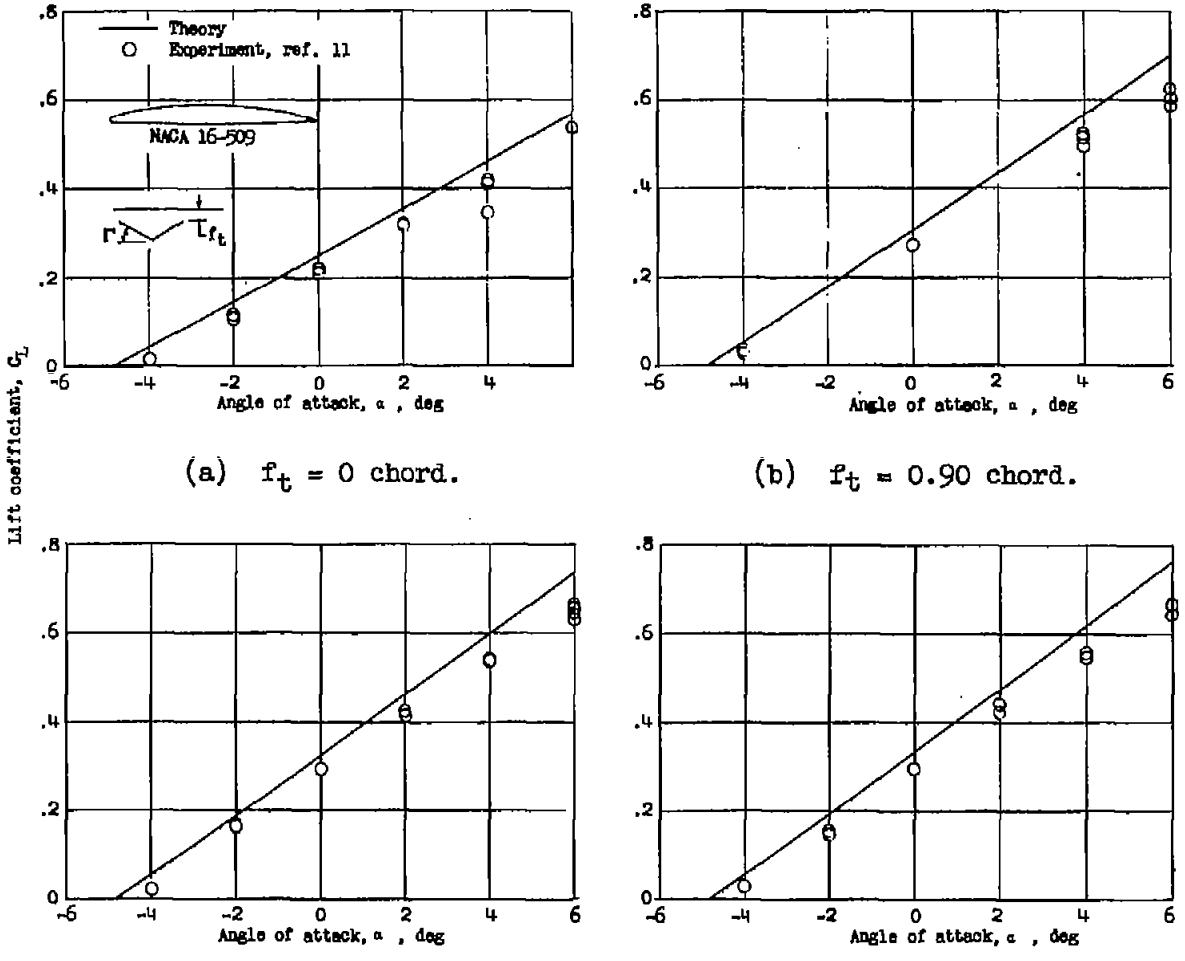

Figure 13.- Comparison of experimental and theoretical lift coefficients for a hydrofoil of aspect ratio 6 with 20° dihedral.

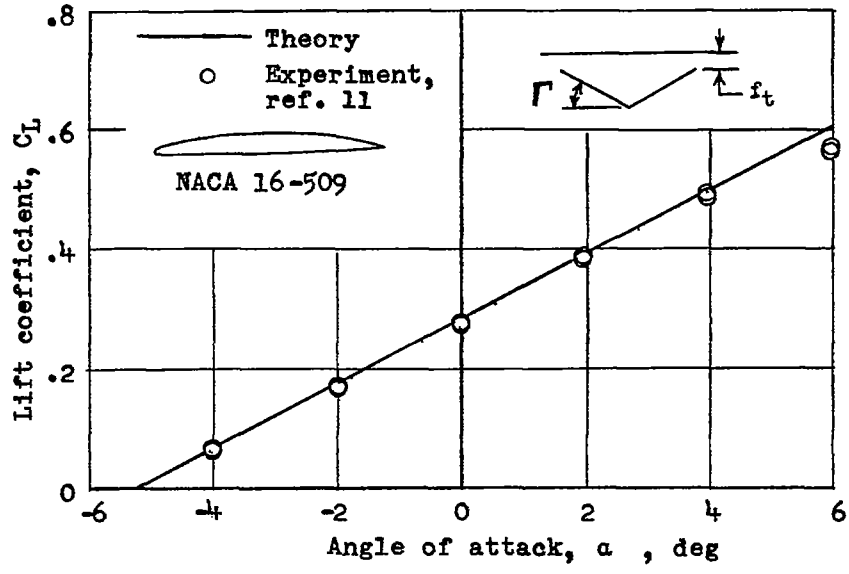

(a) f_t = 0 chord.

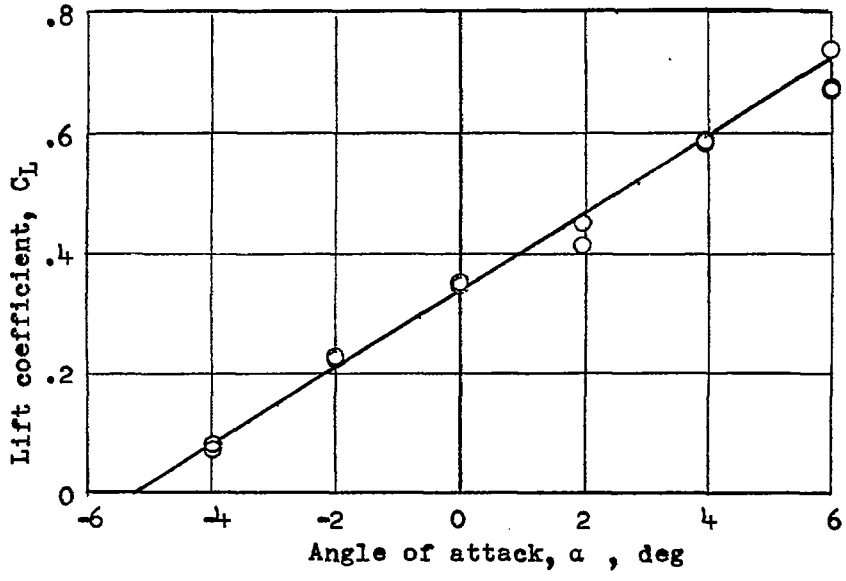

(b) f_t = 3.26 chords.

Figure 14.- Comparison of experimental and theoretical lift coefficients for a hydrofoil of aspect ratio 6 with 30° dihedral.

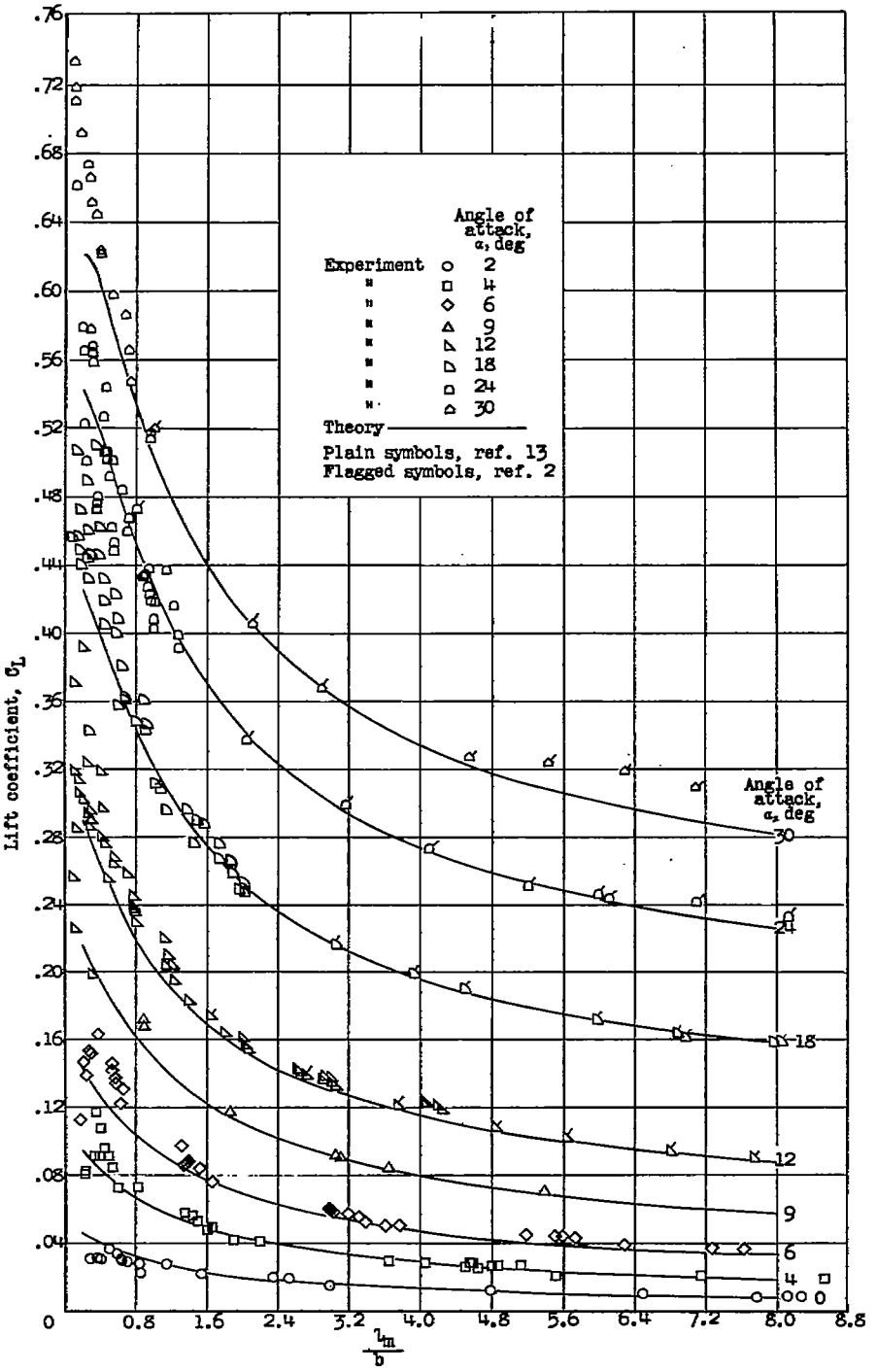

Figure 15.- Comparison of experimental and theoretical lift coefficients for a flat-bottom lifting surface in the planing condition.

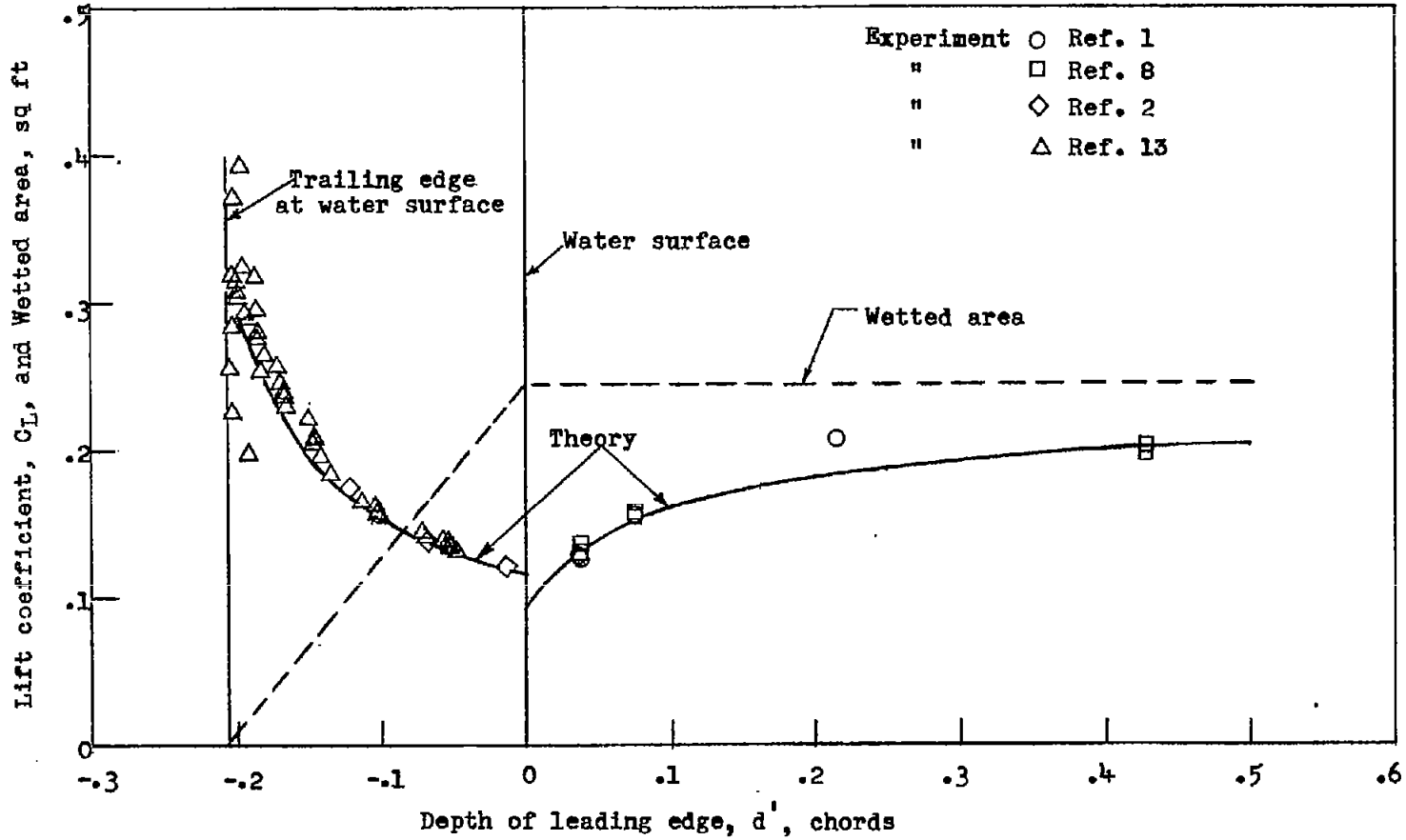

Figure 16.- Variation of theoretical and experimental values of lift coefficient with depth of leading edge of a flat plate of aspect ratio 0.25 at an angle of attack of 12°.